




Novel Keap1-Nrf2 Protein-Protein Interaction Inhibitor UBE-1099 Ameliorates Progressive Phenotype in Alport Syndrome Mouse Model

Shota Kaseda,^{1,2} Yuya Sannomiya,¹ Jun Horizons,¹ Jun Kuwazuru ¹ Mary Ann Suico ^{1,3} Sayaka Ogi,⁴ Ryoko Sasaki,¹ Hidetoshi Sunamoto,⁴ Hirohiko Fukiya,⁴ Hayato Nishiyama,⁴ Misato Kamura,^{1,2} Saki Niinou,¹ Yuimi Koyama,¹ Futoshi Nara,⁴ Tsuyoshi Shuto,^{1,3} Kazuhiro Onuma,⁴ and Hirofumi Kai ^{1,2,3}

Key Points

- UBE-1099 inhibits Keap1-Nrf2 protein-protein interaction and induces Nrf2 activation.
- UBE-1099 ameliorates the progressive phenotype of an Alport syndrome mouse model.
- Keap1-Nrf2 protein-protein interaction inhibitor could be a therapeutic drug for glomerulosclerosis and chronic kidney disease.

Abstract

Background Bardoxolone methyl activates nuclear factor erythroid 2–related factor 2 (Nrf2) *via* covalent binding and irreversible inhibition of Kelch-like ECH-associated protein 1 (Keap1), the negative regulator of Nrf2. Ongoing clinical trials of bardoxolone methyl show promising effects for patients with CKD. However, the direct inhibition of Keap1-Nrf2 protein-protein interaction (PPI) as an approach to activate Nrf2 is less explored.

Methods We developed a noncovalent Nrf2 activator UBE-1099, which highly selectively inhibits Keap1-Nrf2 PPI, and evaluated its efficacy on the progressive phenotype in an Alport syndrome mouse model (*Col4a5-G5X*).

Results Similar to bardoxolone methyl, UBE-1099 transiently increased proteinuria and reduced plasma creatinine in Alport mice. Importantly, UBE-1099 improved the glomerulosclerosis, renal inflammation, and fibrosis, and prolonged the life span of Alport mice. UBE-1099 ameliorated the dysfunction of Nrf2 signaling in the renal tissue of Alport mice. Moreover, transcriptome analysis in the glomerulus showed that UBE-1099 induced the expression of genes associated with the cell cycle and cytoskeleton, which may explain its unique mechanism of improvement such as glomerular morphologic change.

Conclusions UBE-1099 significantly ameliorates the progressive phenotype in Alport mice. Our results revealed the efficacy of Keap1-Nrf2 PPI inhibitor for glomerulosclerosis and present a potential therapeutic drug for CKD.

KIDNEY360 3: 687–699, 2022. doi: <https://doi.org/10.34067/KID.0004572021>

Introduction

Nuclear factor erythroid 2–related factor 2 (Nrf2) is an essential transcription factor that regulates various genes involved in biologic defense (1,2). Under basal condition, Nrf2 is anchored in the cytoplasm by Kelch-like ECH-associated protein 1 (Keap1), an adaptor protein for Cullin-3 ubiquitin ligase, and undergoes proteasomal degradation (3,4). But in the presence of oxidative stress, electrophiles, or itaconate, the reactive cysteine residues of Keap1 are modified. This results in a structural change at the Nrf2 binding site, which allows Nrf2 to translocate to the nucleus and induces target gene transcription (5,6). Enhancement of biologic

defense *via* activation of Nrf2 is expected as a possible novel therapeutic strategy for various intractable diseases (7).

Bardoxolone methyl (CDDO-Me) is an electrophilic agent that induces Nrf2 activation by irreversibly and covalently binding to the cysteine residue of Keap1 (8). Multiple clinical studies have shown that CDDO-Me significantly increases the eGFR in patients with Stage 3–4 CKD (9–11). Although heart failure (HF) events most likely caused by fluid overload occurred in patients with B-type natriuretic peptide levels >200 pg/ml and in patients with a history of hospitalization for HF (11,12), CDDO-Me was well tolerated, and no

¹Department of Molecular Medicine, Graduate School of Pharmaceutical Sciences, Kumamoto University, Kumamoto, Japan

²Program for Leading Graduate School “HIGO (Health Life Science: Interdisciplinary and Global Oriented) Program,” Kumamoto University, Kumamoto, Japan

³Global Center for Natural Resources Sciences, Faculty of Life Sciences, Kumamoto University, Kumamoto, Japan

⁴Pharmaceuticals Research Laboratory, UBE Industries Ltd., Yamaguchi, Japan

Correspondence: Kazuhiro Onuma, UBE Industries Ltd., 1978-5, Kogushi, Ube City 755-8633, Japan, or Hirofumi Kai, Kumamoto University, 5-1 Oe-honmachi, Chuo-ku, Kumamoto City 862-0973, Japan. Email: 32726u@ube-ind.co.jp or hirokai@gpo.kumamoto-u.ac.jp

serious side effects were observed in patients without these risk factors (10). In this context, CDDO-Me is currently in clinical trials for different forms of CKD with careful monitoring and patient selection. Importantly, based on the efficacy and safety data from the CARDINAL phase 3 clinical trial, the Food and Drug Administration (FDA) has now accepted for filing the New Drug Application of CDDO-Me for the treatment of patients with Alport syndrome. Thus, there is a global trend to apply Nrf2 activators to CKD treatment. However, because covalent Keap1 inhibitors such as CDDO-Me have many off-targets involved in the efficacy, it is unclear to what extent their efficacy depends on Nrf2 activation. This is one of the compelling reasons to explore other strategies to activate Nrf2.

The development of Keap1-Nrf2 protein-protein interaction (PPI) inhibitor has been regarded as an innovative strategy to activate Nrf2 (13,14). Unlike the traditional Nrf2 activators such as electrophilic agents, this type of compound induces Nrf2 activation by competitively and directly inhibiting Keap1-Nrf2 PPI in a noncovalent manner (15). This mechanism of action can enhance the selectivity of the agents and reduce the risk of side effects (8).

In this study, we developed UBE-1099, a novel reversible and orally available Keap1-Nrf2 PPI inhibitor, and evaluated its efficacy in a CKD mouse model. Most previous reports conducted short-term studies with an acute model to evaluate the effect of rodent tolerable CDDO-Me analog (CDDO-Im or RTA 405) (16,17) or Keap1-Nrf2 PPI inhibitor (CPUY192018) (18). Here, to assess the long-term effect of Keap1-Nrf2 PPI inhibitor, we utilized an Alport syndrome mouse model, which has a nonsense mutation at glycine 5 in type IV collagen alpha 5 (*Col4a5*-G5 \times) and exhibits clinical phenotypes of CKD (19). Alport mice spontaneously start to show proteinuria and glomerulosclerosis at 8–12 weeks old and renal inflammation and fibrosis at 16 weeks old. These mice die at 35 weeks old. Here, we show that, delivered orally, UBE-1099 strongly induced Nrf2 activation in murine kidney. Notably, treatment with UBE-1099 ameliorated renal pathologies such as glomerulosclerosis, inflammation, and fibrosis, and prolonged the life span of Alport mice.

Materials and Methods

Fluorescence Polarization Assay

Seventy microliters of varying concentrations of UBE-1099, CDDO-Me, or CDDO-Im was added to 350 μ l of buffer solution (20-mM Tris-HCl; 150-mM NaCl; 0.05% Tween 20; 5-mM DTT) containing 6 nM FITC-labeled Nrf2 peptide (Invitrogen) and 0.2 mg/ml BSA. Then, 120 μ l of solution was added to a 96-well plate and mixed with 80 μ l of buffer solution containing 2.5 nM of human KEAP1-GST fusion protein (Ag0779; Proteintech). After incubation at room temperature for 30 minutes, fluorescence polarization was measured at $\lambda_{\text{ex}}=482$ nm and $\lambda_{\text{em}}=530$ nm. The inhibition rate was calculated using the following equation:

$$\text{Inhibition rate (\%)} = 100 - \left[\frac{(A_{\text{sample}} - A_{\text{negative control}})}{(A_{\text{positive control}} - A_{\text{negative control}})} \right] \times 100.$$

Wells without compound were used as a positive control, and wells without Keap1 were used as a negative control.

Animals and *In Vivo* Treatment

The X-linked Alport syndrome mouse model (*Col4a5*^{tm1Yseg} G5X mutant) has been described previously (19). These mice were obtained from the Jackson Laboratory. Age-matched wild-type (WT) C57BL/6 mice (Charles River Laboratories) were used for experiments as controls to compare with Alport mice. Mice were housed in clean vivarium and fed with food and water *ad libitum*. For experiments, male mice were used to eliminate sex difference due to sex-linked inheritance of *Col4a5*^{tm1Yseg} G5X mutation as we did previously (20–24). Six-week-old WT and Alport mice were treated with methylcellulose (vehicle) or UBE-1099 (30 mg/kg per day by mouth) for 16 weeks. UBE-1099 was synthesized by the pharmaceuticals research laboratory at UBE Industries Ltd.

Plasma Pharmacokinetics

Plasma samples were collected 1, 4, 6, 14, and 24 hours after compound administration in BALB/c mice. After adding one volume of acetonitrile and four volumes of acetonitrile containing an internal standard, the mixture was shaken at 750 rpm for 1 minute and centrifuged at 1500 \times g for 2 minutes to remove proteins. The compound concentration in plasma was measured under the following conditions using liquid chromatography tandem mass spectrometry (Shimadzu Corp.): column=Phenomenex Kinetex C18 (50 \times 2, 1 mm, 2.6 μ m), column temperature=40°C, flow velocity=0.3 ml/min, mobile phase A=0.1% formic acid/MiliQ aqueous solution, mobile phase B=0.1% formic acid, 50% acetonitrile/methanol solution, gradient=0–2 minutes; A/B=90/10–10/90, 2–3 minutes; A/B=10/90, 3–3.01 minutes; A/B=10/90–90/10, MS=3200QTrap (Sciex), ionization=ESI, mode=Positive.

GFR and Blood Pressure Measurements

GFR in 22-week-old mice was assessed *via* measurement of the clearance of FITC-sinistrin using a transdermal probe as previously described (16). In brief, mice anesthetized with isoflurane were injected with 7.5 mg/100 g body weight FITC-sinistrin (Medibeacon GmbH) through the subclavian vein. A transdermal GFR monitor was affixed directly to shaved skin on the dorsum of the animal (Medibeacon), and levels of FITC-sinistrin were measured. Calculation of GFR was performed with Medibeacon software according to previously published methods (25). Heart rate, systolic blood pressure (BP), diastolic BP, and mean BP were measured using a noninvasive tail-cuff apparatus (BP-98A-I; Softron) according to the manufacturer's protocol.

Measurement of Proteinuria and Albuminuria Score

Mouse urine samples were collected for 24 hours once every 2 weeks using a metabolic cage (AS ONE Corp.). Urinary protein, albumin, and creatinine were measured using the Bradford method (Bio-Rad), ELISA method (Fujifilm), and Jaffe's method (Wako Pure Chemicals), respectively, as described previously (22). Urinary protein and albumin concentration were normalized with urinary creatinine concentration and presented as proteinuria and albuminuria.

Measurement of Plasma Creatinine and BUN

Mouse blood samples obtained from abdominal aorta were centrifuged at $800\times g$ at $4^{\circ}C$ for 15 minutes, and blood plasma was collected. Plasma creatinine and BUN were measured with DRI-CHEM (Fujifilm) and 7180 biochemistry automatic analyzer (Hitachi), respectively.

Histologic Analysis

Kidney tissues were fixed in 10% formalin and embedded in paraffin. Tissue blocks were sliced at a thickness of $4\ \mu m$ using a microtome and stained with periodic acid–Schiff and Masson's trichrome (MT) as previously described (20,22,23). We evaluated the glomerulosclerosis score as we did previously. More than 100 random glomeruli per mouse were scored based on the following criteria: 0, no lesion; 1, expansion of mesangial area; 2, expansion of Bowman's epithelial cells, adhesion of glomeruli and Bowman's capsule, and partial sclerosis; 3, sclerotic area in 50%–75% of glomeruli; and 4, sclerotic area in 75%–100% of glomeruli. For renal fibrosis, the MT-positive area was quantified using a BZ-X700 microscope and image analysis software (Keyence).

Immunostaining

For immunohistochemistry, $4\text{-}\mu m$ paraffin sections were stained with anti-F4/80 antibody (clone Cl:A3–1; Bio-Rad) and anti-Wilms' tumor 1 (WT1) antibody (clone C-19; Santa Cruz Biotechnology) as previously described (22). The F4/80-positive area in the cortex of the kidney tissue was quantified using a BZ-X700 microscope and image analysis software (Keyence). WT1-positive cells in more than 100 random glomeruli per mouse were counted and expressed as the average per glomerulus.

Immunoblotting

To isolate the whole cell protein, kidney samples were lysed in T-PER Tissue Protein Extraction Reagent (Thermo Fisher Scientific) according to the manufacturer's protocol. To isolate the nuclear protein, kidney samples were homogenized with Dounce homogenizer (D8938; Sigma–Aldrich)

in 2 ml of ice-cold Nuclei EZ Lysis buffer (NUC101; Sigma–Aldrich) and incubated on ice for 5 minutes with an additional 2 ml of lysis buffer. The digested kidneys were passed through a $40\text{-}\mu m$ cell strainer and centrifuged at $500\times g$ at $4^{\circ}C$ for 5 minutes. The pellet was re-suspended and washed with 4 ml of the lysis buffer and incubated on ice for 5 minutes. After passing through a $20\text{-}\mu m$ cell strainer and centrifugation at $500\times g$ at $4^{\circ}C$ for 5 minutes, the pellet was lysed in RIPA buffer (50-mM Tris-HCl, 150-mM NaCl, 1% w/v Nonidet P-40, 0.5% w/v sodium deoxycholate, 0.5% w/v SDS). Protein lysates were subjected to SDS-PAGE and Western blot analysis as described previously (20,22,23). Anti-NRF2 (ab31163) and anti-NQO1 antibodies (ab34173) were from Abcam. Anti-vinculin (ab129002; Abcam) and anti-HDAC2 antibodies (sc-7899; Santa Cruz Biotechnology) were used as loading control. The above primary antibodies were detected using their respective horseradish peroxidase-conjugated secondary antibodies. Super Signal West Pico PLUS Chemiluminescent Substrate (Thermo Fisher Scientific) was used to visualize the blots.

Real-Time Quantitative RT-PCR

Total RNA was isolated from murine kidneys using NucleoSpin RNA (Takara) with homogenization. Reverse transcription and PCR amplification were performed using a PrimeScript RT Reagent Kit with gDNA Eraser and SYBR Premix ExTaq II (Takara), respectively, according to the manufacturer's recommended protocol. The sequences of primers used for quantitative PCR are listed in Table 1.

Isolation of Glomeruli

Glomeruli were isolated using magnetic beads after administration of the compound to Alport mice for 4 weeks from 6 to 10 weeks of age. Briefly, mice were perfused with 38 ml of prewarmed HBSS and 2 ml HBSS with enzymatic digestion solution (300 IU/ml Collagenase type II [Sigma–Aldrich], 1 mg/ml Proteinase E [Sigma–Aldrich], and 50 IU/ml Dnase I [Invitrogen]). Then, kidneys were removed and minced into 1-mm^3 pieces, and digested in

Table 1. Primers used in quantitative RT-PCR

Gene	Sense	Antisense
<i>Nqo1</i> ^a	5'-CAGCCAATCAGCGTTCGGTA-3'	5'-CTTCATGGCGTAGTTGAATGATGTC-3'
<i>Gapdh</i> ^a	5'-TGTGTCCGTCGTGGATCTGA-3'	5'-TTGCTGTTGAAGTCGCAGGAG-3'
<i>Lcn2</i>	5'-CAGAAGGCAGCTTTACGATG-3'	5'-CCTGGAGCTTGGAAACAAATG-3'
<i>Kim1</i>	5'-GGAAGTAAAGGGGGTAGTGGG-3'	5'-AAGCAGAAGATGGGCATTGC-3'
<i>Tgf-β</i>	5'-CACCTGCAAGACCATCGACAT-3'	5'-GAGCCTTAGTTTGACAGGATCTG-3'
<i>IL-1β</i>	5'-GCTGAAAGCTCTCCACCTCAATG-3'	5'-TGTCGTTGCTTGGTTCTCCTTG-3'
<i>Mcp1</i>	5'-GAAGCTGTAGTTTTGTCAACCAAG-3'	5'-AGGTAGTGGATGCATTAGCTTCA-3'
<i>Tnfa</i>	5'-CATCTTCTCAAAAATTCGAGTGACAA-3'	5'-TGGGAGTAGACAAGGTACAACCC-3'
<i>Mmp9</i>	5'-GGACCCGAAGCGGACATTG-3'	5'-CGTCGTCGAAATGGGCATCT-3'
<i>Il-6</i>	5'-GAGGATACCACTCCCAACAGACC-3'	5'-AAGTGCATCATCGTTGTTTCATACA-5'
<i>Nrf2</i>	5'-CACTCCAGCGAGCAGGCTAT-3'	5'-CTGGGACTGTAGTCTGGCG-3'
<i>Nqo1</i> ^b	5'-TTCTGTGGCTTCCAGGTCTT-3'	5'-AGGTGCTTGGAGCAAAATA-3'
<i>Gclc</i>	5'-GGACAAACCCCAACCATCC-3'	5'-GTTGAACTCAGACATCGTTCCT-3'
<i>Gapdh</i> ^b	5'-CCTGGAGAAACCTGCCAAGTATG-3'	5'-GGTCCTCAGTGTAGCCCAAGATG-3'

^aUsed in Figure 1.

^bUsed in Figures 2, 4, and 5.

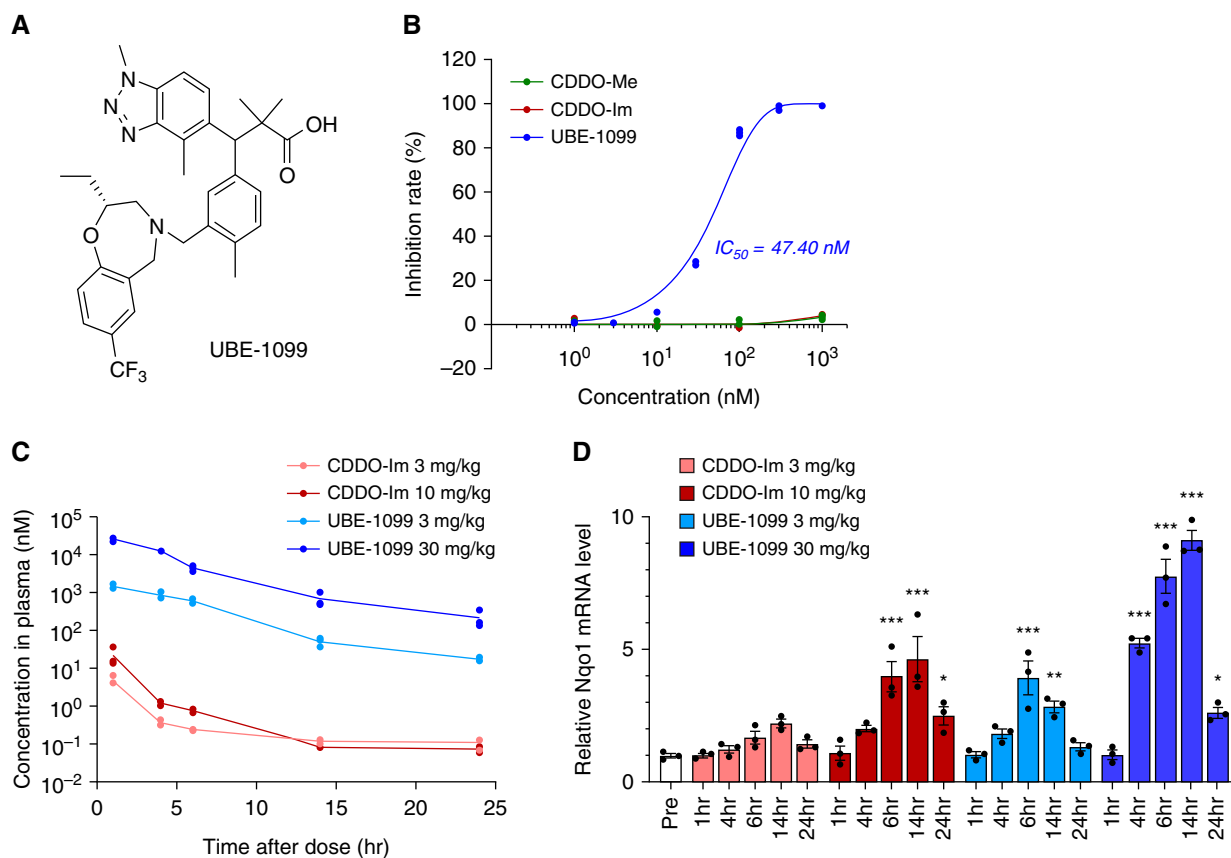


Figure 1. | UBE-1099 induced nuclear factor erythroid 2-related factor 2 (Nrf2) activation through the inhibition of Kelch-like ECH-associated protein 1 (Keap1)-Nrf2 protein-protein interaction. (A) Chemical structure of UBE-1099. (B) Keap1-Nrf2 protein-protein interaction was measured by fluorescence polarization assay. (C) Plasma samples were collected at the indicated time points, and concentrations of CDDO-Im and UBE-1099 were measured by liquid chromatography tandem mass spectrometry. (D) Total RNA was isolated from renal tissues at the indicated time points. The level of the Nqo1 mRNA was measured and normalized to the level of Gapdh mRNA (internal control). Data are presented as the mean \pm SEM ($n=3$ per group). P values were assessed by Dunnett's test. * $P<0.05$, ** $P<0.01$, *** $P<0.001$ versus Pre.

2 ml enzymatic digestion buffer at 37°C for 20 minutes on a rotator. The digested kidneys were passed through a 200- μ m cell strainer, and glomeruli were washed four times and collected using Dynabeads (Invitrogen) according to the manufacturer's recommended protocol.

RNA Sequencing

Total RNA from glomeruli was isolated and purified using the RNeasy plus Mini Kit (Qiagen) according to the manufacturer's instructions. The purity and integrity of the isolated RNA was checked with an Epoch Microplate Spectrophotometer (BioTek) and Agilent 2100 BioAnalyzer. Poly(A)-selected cDNA libraries were generated using the TruSeq Stranded mRNA Library Prep kit (Illumina). Sequencing was performed using NextSeq500 system (Illumina) in a 76-bp single-end read. After adaptor trimming and quality check by Trim Galore (v0.5.0), sequencing reads were aligned to the mouse reference genome (mm10) using STAR (v2.6.0a). Gene expression profiles for each sample were measured as transcripts per million (TPM) using RSEM (v1.3.1). For differentially expressed genes, fold changes of >1.2 or <-1.2 ($P<0.05$; WT versus Alport vehicle, Alport vehicle versus Alport UBE-1099) were

measured using DESeq2 and subjected to heatmap analysis. TPM data were subjected to Gene Set Enrichment Analysis (v4.1.0). The RNA-seq data have been deposited in the DNA Data Bank of Japan (DDBJ) Sequence Read Archive under accession number DRA012265.

Statistical Analyses

All data are presented as the mean \pm SEM. The significance of the difference between two groups was assessed using Student's unpaired two-tailed t test. For three- or four-group comparisons, we used ANOVA with Dunnett's test. P -values <0.05 were considered to be statistically significant.

Study Approval

Animal experiments for Figures 1 and 7 were reviewed and approved by the Animal Care and Use Committee of the pharmaceutical research laboratory of UBE Industries Ltd., Yamaguchi, Japan (P-20032, P-20170). Animal experiments for Figures 2–6 and Supplemental Figures 1–11 were approved by the Animal Care and Use Committee of Kumamoto University, Kumamoto, Japan (A2020–020).

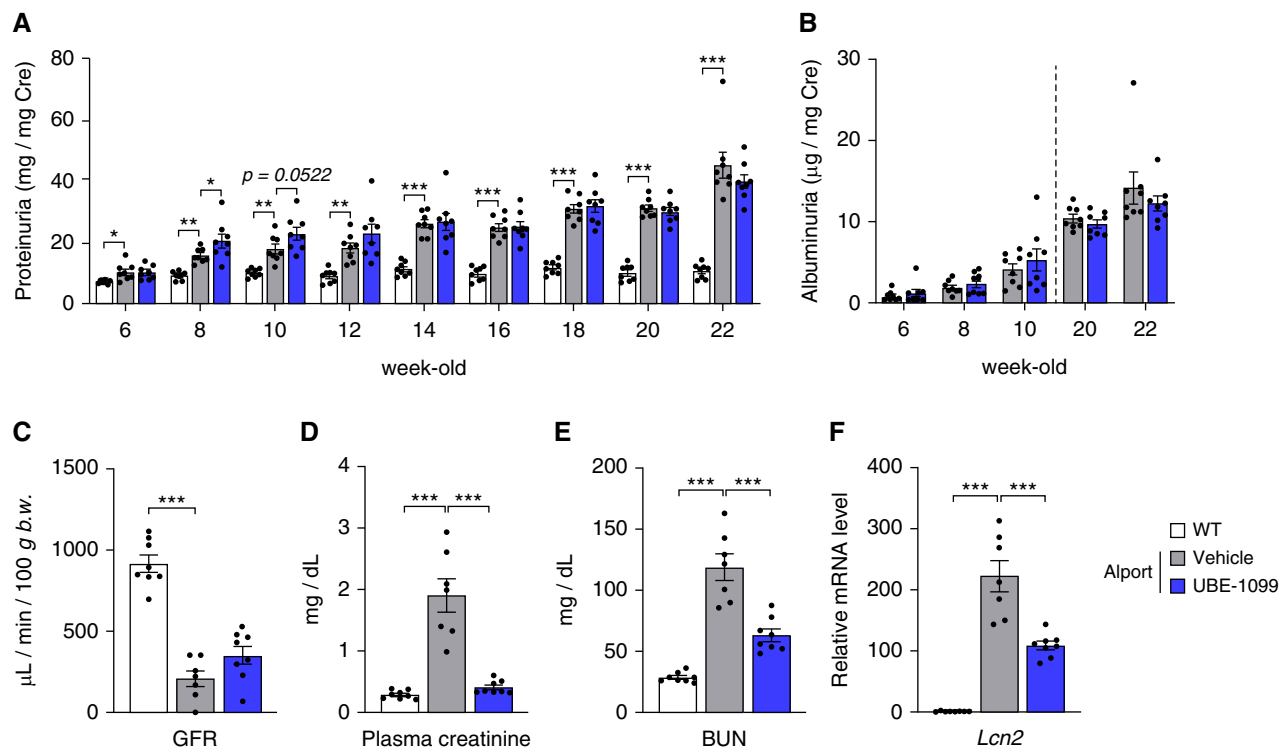


Figure 2. | Effects of UBE-1099 on renal dysfunction in an Alport mouse model. (A) and (B) Urine samples were collected at the indicated time points. Urinary protein and albumin were measured using the Bradford and ELISA methods, respectively. Urinary creatinine was measured using Jaffe's method. Urinary protein and albumin concentration were normalized with urinary creatinine concentration and presented as proteinuria and albuminuria, respectively. (C) GFR was measured with a transdermal GFR monitor (MediBeacon) in 22-week-old wild-type (WT) and Alport mice. (D) and (E) Plasma creatinine and BUN were measured using DRI-CHEM (Fujifilm) and a 7180 biochemistry automatic analyzer (Hitachi), respectively, in 22-week-old WT and Alport mice. (F) Total RNA was isolated from the renal tissue of 22-week-old mice. The level of the *Lcn2* mRNA was measured and normalized to the level of *Gapdh* mRNA (internal control). Data are presented as the mean \pm SEM ($n=7-8$ per group). P values were assessed by Dunnett's test. * $P<0.05$, ** $P<0.01$, *** $P<0.001$.

Results

UBE-1099 Induced Nrf2 Activation through the Inhibition of Keap1-Nrf2 PPI

To develop a noncovalent Nrf2 activator, we performed fluorescence polarization-based screening using the previously developed Keap1-Nrf2 PPI inhibitor (26) as the lead compound, and optimized the structure based on the structure activity relationship. We successfully identified UBE-1099 that markedly inhibited the Keap1-Nrf2 interaction (Figure 1, A and B). CDDO-Me and CDDO-Im did not show an inhibitory effect (Figure 1B) because this evaluation system used the human Keap1-Kelch domain, which does not contain BTB and IVR domain with the cysteine residue that is the target of covalent Nrf2 activator. The maximum blood concentration of UBE-1099 is much higher than that of CDDO-Im when orally administered in mice, and UBE-1099 strongly induced the Nrf2-target molecule, NAD(P)H: quinone oxidoreductase 1 (*Nqo1*) expression in mouse renal tissue (Figure 1, C and D).

Effects of UBE-1099 on Renal Dysfunction in an Alport Mouse Model

The Nrf2-activating effect of UBE-1099 lasted up to 24 hours after administration at a concentration of 30 mg/kg as detected from the elevated expression of *Nqo1* mRNA compared with pretreatment (Figure 1D). Therefore, we set

the dosing condition at 30 mg/kg per day by mouth to maintain a constant effect and assessed the effect of UBE-1099 on the renal function in Alport mice at 6–22 weeks old. Slight weight loss and increased urine volume were observed in the UBE-1099-treated Alport mice, but no noticeable toxicity was suspected (Supplemental Figure 1). UBE-1099 also did not induce changes in heart rate or BP in Alport mice over time (Supplemental Figure 2). Similar to the results in clinical trials of CDDO-Me (27), UBE-1099 transiently increased the proteinuria but not albuminuria in Alport mice at 2–4 weeks after the start of administration (Figure 2, A and B; 8 and 10 weeks old). However, at the late stage of the disease, UBE-1099 slightly, although not statistically, reduced the proteinuria and albuminuria in Alport mice (Figure 2, A and B; 22 weeks old). Although a clear improvement in GFR was not confirmed, UBE-1099 significantly decreased plasma creatinine and BUN in Alport mice (Figure 2, C-E). Moreover, the mRNA expression level of the renal injury marker Lipocalin-2 (*Lcn2*; also known as NGAL) was statistically decreased by treatment with UBE-1099 (Figure 2F).

UBE-1099 Suppressed the Glomerulosclerosis in an Alport Mouse Model

We investigated the effect of UBE-1099 on glomerulosclerosis, which is one of the hallmarks of Alport syndrome.

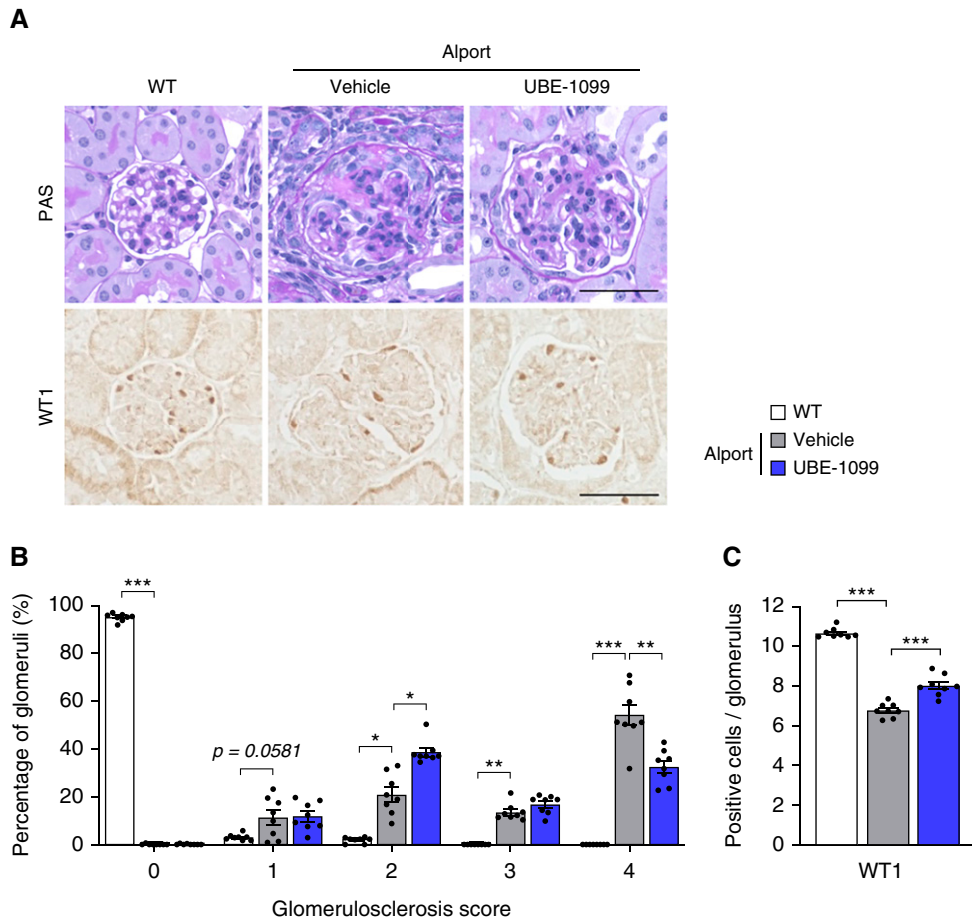


Figure 3. | UBE-1099 suppressed glomerulosclerosis in an Alport mouse model. (A) Renal sections of 22-week-old WT and Alport mice were analyzed by periodic acid-Schiff (PAS) staining and immunohistochemistry of Wilms' tumor 1 (WT1). Representative images are shown. Scale bars: 50 μ m. (B) Glomerulosclerosis scores were evaluated based on the PAS-stained sections. See Materials and Methods for assessment. (C) Quantification of WT1-positive cells in the glomerulus. Data are presented as the mean \pm SEM ($n=8$ per group). P values were assessed by Dunnett's test. * $P<0.05$, ** $P<0.01$, *** $P<0.001$.

Although vehicle-treated Alport mice had typical glomerulosclerosis, with the formation of glomerular tuft adhesion in Bowman's capsule, UBE-1099 inhibited the collapse of glomeruli and ameliorated the characteristic glomerulosclerosis (Figure 3A; periodic acid-Schiff). Although >50% of glomeruli showed the highest glomerulosclerosis score (injury score of 4) in vehicle-treated Alport mice, <30% of glomeruli had severe glomerulosclerosis in UBE-1099-treated Alport mice, and 40% of these glomeruli presented a less severe injury score of 2 (Figure 3B). Because the podocyte is the most important cell in glomerular filtration and its injury is associated with glomerulosclerosis (28–30), we evaluated the number of podocytes by staining their nuclear marker, WT1. We found that UBE-1099 suppressed the reduction of WT1-positive cells in glomeruli (Figure 3, A and C). These results collectively revealed that UBE-1099 ameliorated the glomerulosclerosis that is characteristically seen in Alport mice.

UBE-1099 Suppressed Renal Tissue Inflammation and Fibrosis in an Alport Mouse Model

Along with glomerulosclerosis, Alport mice overtly exhibit renal inflammation and fibrosis (20–24). Immunostaining of

F4/80 showed that macrophage infiltrated the cortical area of kidney tissue in Alport mice, but UBE-1099 suppressed it to the level of the WT mice (Figure 4, A and B). MT staining revealed that the fibrotic region in the kidney tissue of Alport mice was reduced by treatment with UBE-1099 (Figure 4, A and C). Consistent with the staining results, the expression levels of inflammatory cytokines (*Mcp1*, *Il-1 β* , *Il-6*, and *Tnf- α*) and fibrosis-related genes (*Tgf- β* and *Mmp9*) were downregulated by treatment with UBE-1099 (Figure 4, D–I). Moreover, kidney injury marker-1 (*Kim1*) was downregulated by UBE-1099 (Figure 4J). These results suggest that UBE-1099 suppressed renal tissue injury, inflammation, and fibrosis in Alport mice.

UBE-1099 Induced Nrf2 Activation and Ameliorated the Dysfunction of Nrf2 Signaling in the Renal Tissue of an Alport Mouse Model

Oxidative stress is one of the leading causes of progression of CKD (31,32), and the Nrf2 signaling pathway is an evolutionally conserved intracellular defense mechanism against oxidative stress (1,2). So, we isolated whole cell protein or nuclear fraction protein from murine kidney tissues and assessed the expression level of Nrf2 and its

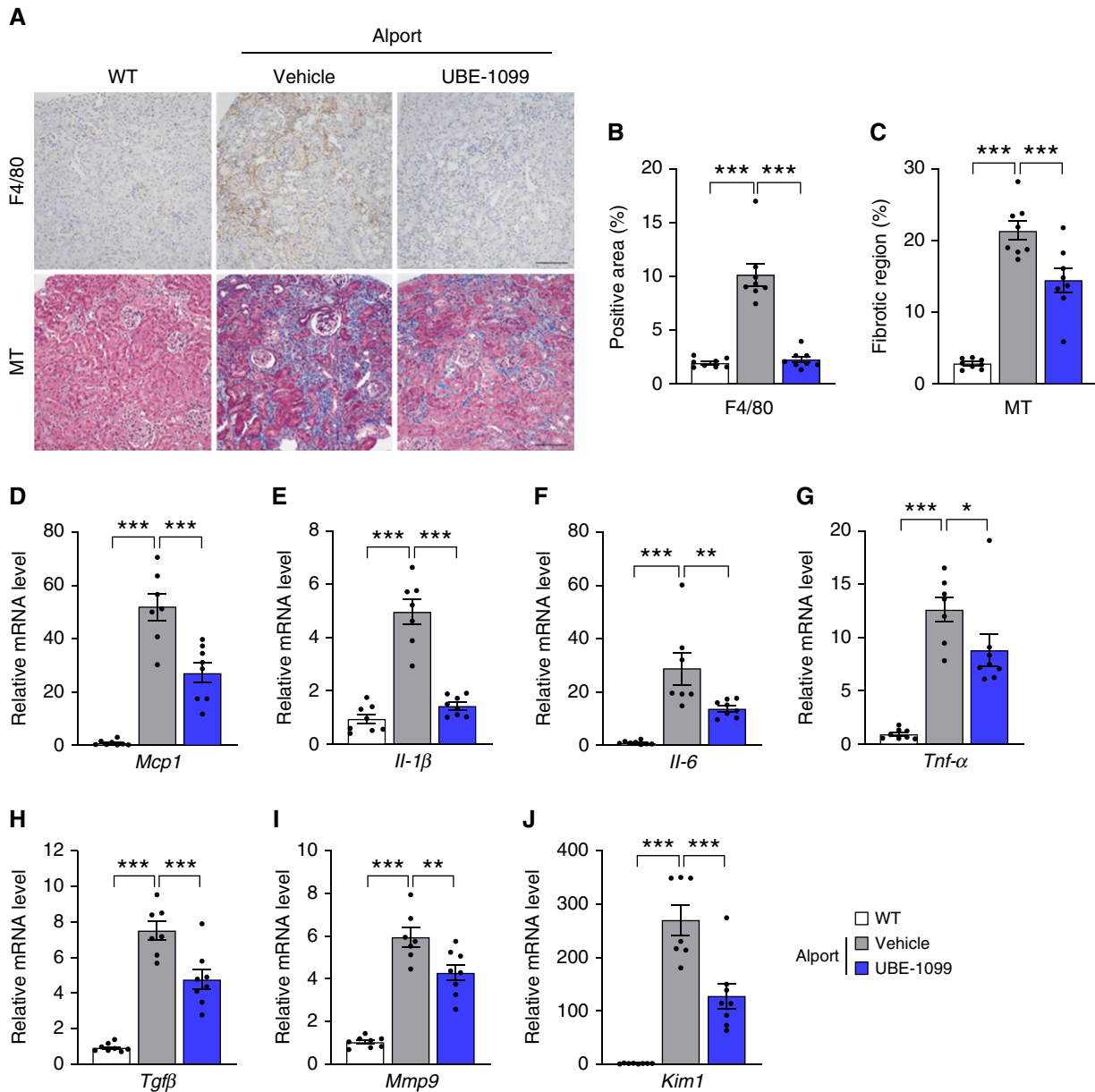


Figure 4. | UBE-1099 suppressed renal tissue inflammation and fibrosis in an Alport mouse model. (A) Renal sections of 22-week-old WT and Alport mice were analyzed using F4/80 immunohistochemistry and Masson's trichrome (MT) staining. Representative images are shown. Scale bars: 200 μ m. (B) and (C) F4/80-positive area and fibrotic region were evaluated based on the F4/80-stained section and MT-stained section, respectively, using Bio-Revo imaging and analysis software. (D–J) Total RNA was isolated from renal tissues of 22-week-old WT and Alport mice. The level of the indicated mRNA was measured and normalized to the level of *Gapdh* mRNA (internal control). Data are presented as the mean \pm SEM ($n=7$ –8 per group). P values were assessed by Dunnett's test. * $P<0.05$, ** $P<0.01$, *** $P<0.001$.

downstream targets. Compared with WT, Alport murine kidney exhibited dysregulation of the protein expression of Nrf2 and its downstream molecules, NQO1 (Figure 5, A, C, and D). The protein expression level of Nrf2 was slightly increased, and NQO1 was highly increased in the kidney of UBE-1099-treated Alport mice compared with vehicle-treated Alport mice. Because active Nrf2 localizes to the nucleus, we examined Nrf2 expression in kidney nuclear extracts. Nrf2 protein expression was increased in the nuclear extracts of UBE-1099-treated Alport mice to a level

similar to that of WT mice, whereas the nuclear Nrf2 protein level remained low in untreated Alport mice (Figure 5, B and E). The mRNA expression level of *Nrf2* was reduced and normalized to WT level in Alport mice treated with UBE-1099 compared with vehicle (Figure 5F). Notably, the expression of the Nrf2-induced antioxidant molecules was also increased at the transcription level (Figure 5, G and H). Collectively, these data suggest that UBE-1099 activates Nrf2 signaling and ameliorates the dysregulation of the Nrf2 signaling pathway in Alport mice.

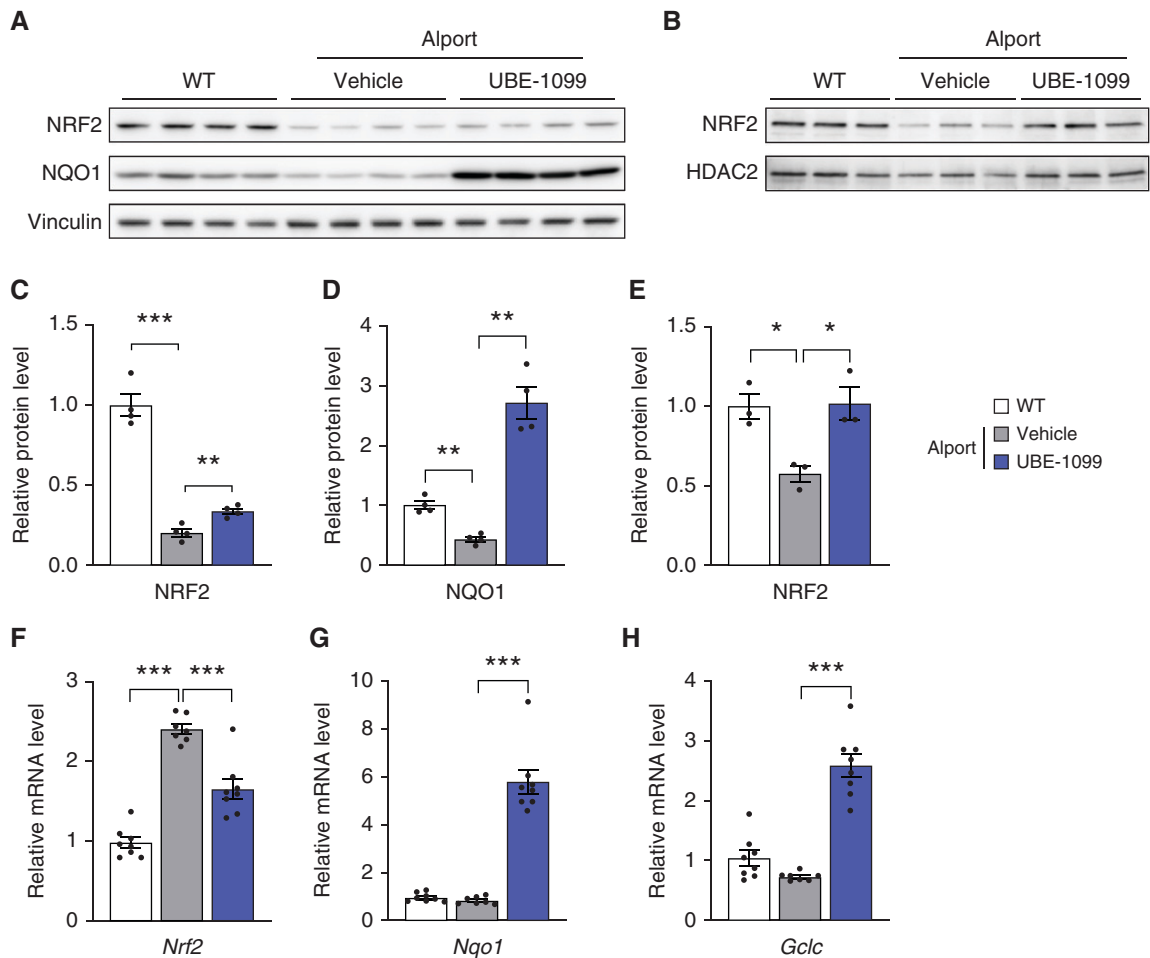


Figure 5. | UBE-1099 induced Nrf2 activation and ameliorated the dysfunction of Nrf2 signaling in the renal tissue of an Alport mouse model. (A) Whole cell protein and (B) nuclear fraction protein were isolated from kidney tissue in the indicated group at 22 weeks of age and were analyzed by immunoblotting. The full-length blots are presented in Supplemental Figure 13. (C–E) The relative amount of proteins was quantified using Image Gauge software (Fujifilm) and normalized with Vinculin and HDAC2 (internal control). Data are presented as the mean \pm SEM ($n=3-4$ per group). P values were assessed by Dunnett's test. * $P<0.05$, ** $P<0.01$, *** $P<0.001$. (F–H) Total mRNA was isolated from renal tissues of 22-week-old WT or Alport mice. The level of the indicated mRNA was normalized to the level of *Gapdh* mRNA (internal control). Data are presented as the mean \pm SEM ($n=7-8$ per group). P values were assessed by Dunnett's test. *** $P<0.001$.

Transcriptome Analysis Reveals the Comprehensive Effects of UBE-1099 in the Glomeruli of an Alport Mouse Model

To clarify the molecular effects of UBE-1099 on glomerulosclerosis in Alport mice, we performed RNA sequencing on the glomeruli of WT and Alport mice treated with vehicle or UBE-1099 (30 mg/kg per day by mouth) for 4 weeks. Transcriptome analysis showed 3511 genes with differential expression between WT and Alport/vehicle, 633 genes between Alport/vehicle and Alport/UBE-1099 (fold change <-1.2 or >1.2 ; $P<0.05$; Figure 6A). Importantly, more than half of the fluctuated genes between Alport/vehicle and Alport/UBE-1099 are not fluctuated genes between WT and Alport/vehicle (Figure 6A and Supplemental Figure 3). Therefore, we performed gene set enrichment analysis to characterize the altered genes. We detected gene ontology terms associated with endoplasmic reticulum (ER) stress, cell adhesion, and transporter as the main abnormalities in the Alport/vehicle group (Supplemental Figures 4–6). On the other hand, we detected gene ontology terms associated with the cell cycle, Nrf2 signaling, cytoskeleton, and

mitochondria as the target of UBE-1099 (Figure 6B and Supplemental Figures 7–9). It is considered that UBE-1099 activated Nrf2 and acted on the downstream pathway (33–38). It had been suggested previously that the effect of CDDO-Me in increasing the GFR involves changes in glomerular structure (17). Based on this notion and the differential expression of cell cycle and cytoskeletal pathways without changes in cell composition in the glomerulus (Supplemental Figure 10), it is possible that UBE-1099 may also induce glomerular structure change.

UBE-1099 Prolonged the Life Span of an Alport Mouse Model

Because UBE-1099 improved the glomerulosclerosis, renal inflammation, and fibrosis in Alport mice, we investigated whether it prolonged the life span of these mice. We treated Alport mice with UBE-1099 (30 mg/kg per day by mouth) from 6 weeks old and monitored their survival. Although half of the vehicle-treated Alport mice had died

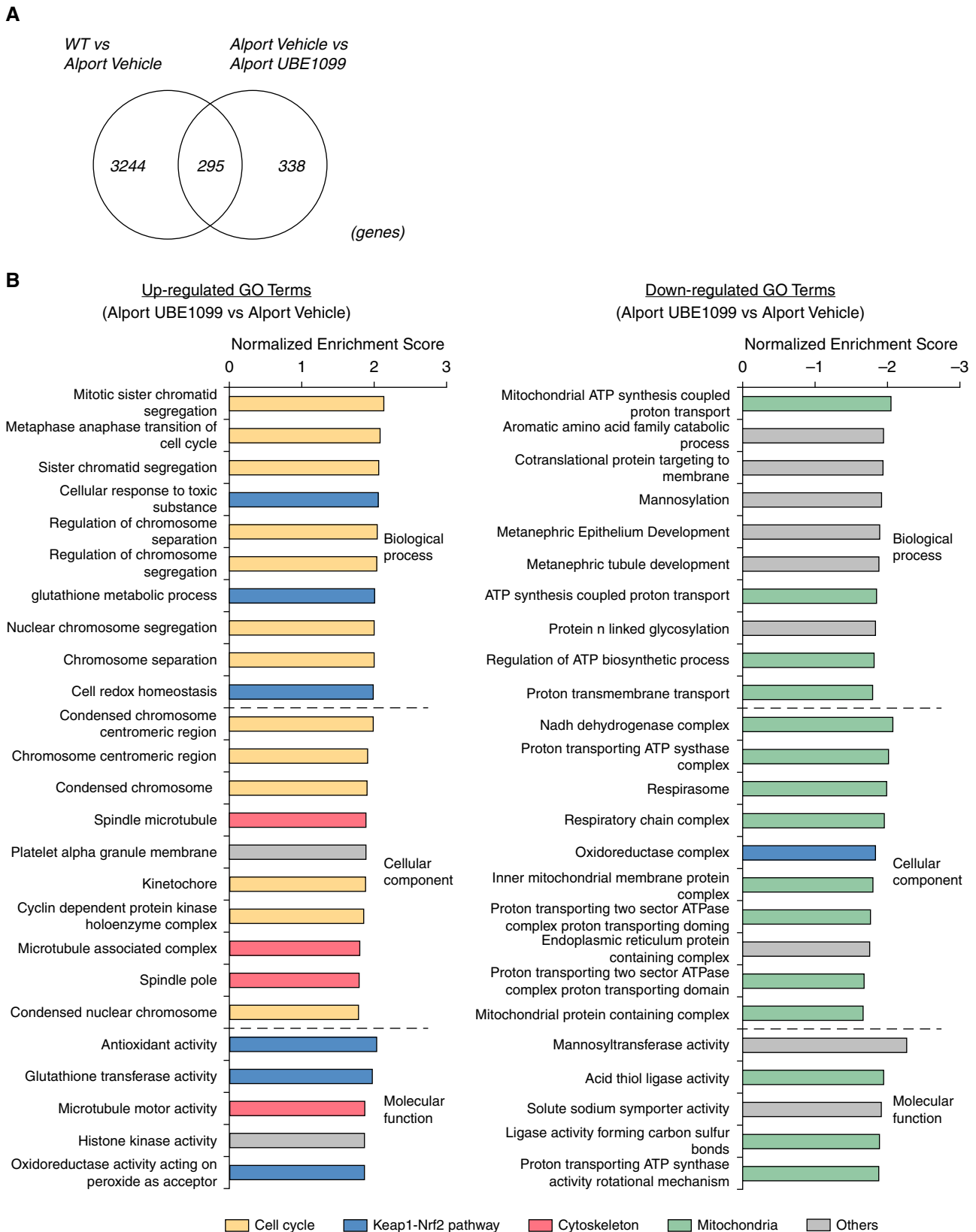


Figure 6. | Transcriptome analysis reveals the comprehensive effects of UBE-1099 in the glomeruli of an Alport mouse model. (A) Venn diagram shows the number of fluctuated genes in three comparisons (WT versus Alport vehicle, Alport vehicle versus Alport UBE-1099; fold change >1.2 or <-1.2, $P < 0.05$). (B) Gene ontology (GO) analysis of the differentially expressed genes in UBE-1099-treated Alport mice versus Alport vehicle analyzed using Gene Set Enrichment analysis software (v4.10). Colored graphs represent the terms as indicated. $P < 0.01$.

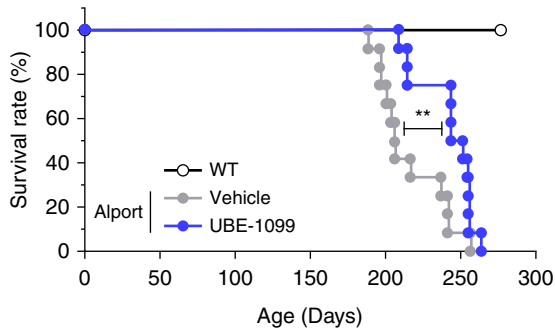


Figure 7. | UBE-1099 prolonged the life span in an Alport mouse model. Kaplan Meier survival curves. Results were derived from WT ($n=12$), vehicle-treated Alport ($n=12$), and UBE-1099-treated Alport mice ($n=12$). P values were assessed by log-rank test. $**P<0.01$.

by 210 days, half of the UBE-1099-treated mice survived beyond 250 days (Figure 7). This result suggests that UBE-1099 delayed the onset of ESKD.

Discussion

This study revealed the efficacy of Keap1-Nrf2 PPI inhibitor on glomerulosclerosis in CKD. Interestingly, although UBE-1099 ameliorated the renal pathology and prolonged the life span of Alport syndrome model mice, a transient increase in proteinuria was confirmed after the start of administration. This is similar to clinically observed phenomenon in patients receiving CDDO-Me (27). It has been suggested that changes in glomerular structure are involved in the improvement of GFR and increase in proteinuria by CDDO-Me (17), but the detailed mechanism is unknown. Our transcriptome analysis of glomeruli revealed that UBE-1099 increased the expression of genes related to the cell cycle and cytoskeleton in the glomerulus of Alport mice. These pathways may contribute to the unique mechanism of CKD improvement by UBE-1099. UBE-1099 increased the antioxidant activity and detoxification process (Figure 6B), which was expected considering that these are target processes of Nrf2 and indicated that UBE-1099 activated the Nrf2 pathway. However, it is surprising that UBE-1099 downregulated the processes associated with ATP production and mitochondrial function (Figure 6B). We previously observed that treatment with MitoQ, which is a mitochondria-targeted antioxidant supplement (39,40), did not improve the glomerulosclerosis of Alport mice (data not shown). Together, these data suggest that the ameliorative effect of UBE-1099 is not merely *via* the suppression of oxidative stress but also involves the regulation of glomeruli cell cycle and cell structure. Moreover, considering that the renal tubules reabsorb most of the primitive urine containing small proteins, UBE-1099 may also act on renal tubules and increase the urine volume and urinary protein by inhibiting reabsorption.

Although there are studies showing the efficacy of activating Nrf2 (41–43), other reports show that Nrf2 activation exacerbates glomerular diseases (16,44). Especially, Rush *et al.* indicated that genetic or pharmacologic Nrf2

activation worsened proteinuria and glomerulosclerosis in an experimental model induced by adriamycin and angiotensin II, whereas Nrf2 knockout mice were protected against proteinuria (16). These results suggest that under certain conditions such as adriamycin-induced injury and high level of angiotensin II, Nrf2 activation exacerbates renal pathology. However, at least to date, there have been no reports of a deterioration of renal function in clinical trials in patients with diabetic kidney disease (AYAME), autosomal dominant polycystic kidney disease (FALCON), IgA nephropathy, type I diabetic nephropathy, focal segmental glomerulosclerosis (PHOENIX), and Alport syndrome (CARDINAL). This suggests that exacerbation events that are provoked in experimental mouse model cannot be extrapolated to humans. Because the Alport mouse model exhibits a phenotype close to the clinical phenotype in that renal function gradually declines over a period of more than half a year, we may have confirmed the ameliorative effect of Nrf2 activator against glomerulosclerosis. We also confirmed that UBE-1099 did not worsen the early renal pathology and did not affect the food intake and muscle weight in Alport mice (Supplemental Figure 11).

Glomerular diseases, including Alport syndrome, are primarily treated with renin-angiotensin system inhibitors (45). Moreover, recent clinical studies show the efficacy of sodium/glucose cotransporter 2 (SGLT2) inhibitors for nondiabetic glomerular disease (46). However, because these medicines are symptomatic treatments, their therapeutic effects are limited and only suppress the decline in renal function. Therefore, the development of drugs that improve renal function, such as CDDO-Me, is essential to prevent the progression of CKD to ESKD. A longer period of treatment with CDDO-Me will clarify its effect on GFR in patients with kidney disease. Considering that the direct effect of increasing Nrf2 and GFR was observed using Nrf2 genetically modified mice in a diabetes model (47), development of Keap1-Nrf2 PPI with higher Nrf2 activity may be expected to improve GFR further.

Importantly, based on the efficacy and safety data from the CARDINAL phase 3 clinical trial, the FDA has now accepted for filing the New Drug Application of CDDO-Me for the treatment of patients with Alport syndrome. Thus, there is a global trend to apply Nrf2 activators to CKD treatment. Exploring other strategies of activating Nrf2, such as using highly specific Keap1-Nrf2 PPI inhibitors that are less likely to cause off-target side effects, could provide safer and more options clinically. The endothelin signaling is suggested to be involved in the side effect of CDDO compounds because HF and fluid retention observed in the BEACON trial were also observed in the clinical trial of endothelin receptor antagonist Avosentan in patients with Stage 3–4 CKD (12,48). Here, we confirmed that CDDO-Im significantly and dose dependently decreased endothelin-1 receptor expression. However, UBE-1099 did not affect endothelin-1 expression in proximal tubular epithelial cells (Supplemental Method and Supplemental Figure 12). This suggests that UBE-1099 does not produce an off-target effect similar to CDDO-Im.

Our present study has some limitations. First, we were not able to clarify fully whether our results depend solely on Nrf2. UBE-1099 highly selectively inhibits Keap1-Nrf2

PPI, but we cannot rule out the possibility that it interacts with other targets. To resolve this issue, the use of genetically modified mice, such as Nrf2 knockout mice, is necessary. Additionally, in order to avoid affecting the renal pathology, we measured BP with a noninvasive tail cuff, which may fail to identify small to moderate changes in BP. Therefore, in the future, it may be necessary to measure BP using other methods.

In conclusion, we show that Nrf2 activation by Keap1-Nrf2 PPI inhibitor improved renal pathology and prolonged the survival of Alport mice. These results not only present the efficacy of Keap1-Nrf2 PPI inhibitor for therapeutic application for Alport syndrome and CKD, but also support the current trend toward considering the use of Nrf2 activators for patients with kidney disease.

Disclosures

H. Kai received research funding from Grants-in-Aid for Scientific Research from the Ministry of Education, Sciences, Sports, and Culture (MEXT) of Japan. S. Kaseda received research funding from the Japan Society for the Promotion of Science. T. Shuto reports received research funding from Grants-in-Aid for Scientific Research from the Ministry of Education, Sciences, Sports, and Culture (MEXT) of Japan. All remaining authors have nothing to disclose.

Funding

This work was supported by the Japan Society for the Promotion of Science (JSPS) KAKENHI (grant nos. JP26460098 and JP17K08309 to M.A. Suico, and grant no. JP19H03379 to H. Kai), the Alport Syndrome Research Funding Program of the Alport Syndrome Foundation and the Pedersen family, Kidney Foundation of Canada (to H. Kai), Grant-in-Aid for JSPS Fellows for Young Researchers (grant no. JP19J23608 to S. Kaseda), and the Japan Agency for Medical Research and Development (AMED; grant no. JP21ek0310017 to H. Kai).

Acknowledgment

We thank Mr. Kenichi Komori, Mr. Yasunori Tokunaga, Mr. Shingo Usuki for their technical assistance.

Author Contributions

H. Kai, S. Kaseda, F. Nara, S. Ogi, K. Onuma, T. Shuto, and M.A. Suico designed the research; H. Fukuya, J. Horizono, M. Kamura, S. Kaseda, Y. Koyama, J. Kuwazuru, S. Niinou, S. Ogi, K. Onuma, Y. Sannomiya, R. Sasaki, and H. Sunamoto conducted the experiments; S. Kaseda, K. Onuma, and M.A. Suico wrote the manuscript; H. Nishiyama contributed to the synthesis of UBE-1099; and all authors discussed the results and provided input on the manuscript.

Data Sharing Statement

All data are included in the manuscript and/or supporting information.

Supplemental Material

This article contains supplemental material online at <http://kidney360.asnjournals.org/lookup/suppl/doi:10.34067/KID.0004572021/-/DCSupplemental>.

Supplemental Method. Endothelin-1 concentration measurement.

Supplemental Figure 1. UBE-1099 slightly reduced the body weight and increased the urine volume in Alport mice.

Supplemental Figure 2. UBE-1099 did not affect the heart rate or blood pressure in Alport mice.

Supplemental Figure 3. Transcriptome analysis reveals the comprehensive effects of UBE-1099 in the glomeruli of Alport mice.

Supplemental Figure 4. Dysregulated gene ontology (GO) terms in the glomeruli of Alport mice.

Supplemental Figure 5. Upregulated GO terms for Alport vehicle versus wild type (WT).

Supplemental Figure 6. Downregulated GO terms for Alport vehicle versus WT.

Supplemental Figure 7. Upregulated GO terms for Alport UBE-1099 versus Alport vehicle.

Supplemental Figure 8. Downregulated GO terms for Alport UBE-1099 versus Alport vehicle.

Supplemental Figure 9. UBE-1099 altered genes in each condition.

Supplemental Figure 10. Expression level of cell specific markers in the glomerular cell.

Supplemental Figure 11. UBE-1099 did not affect the food intake and muscle weight in Alport mice and did not worsen the early renal pathology.

Supplemental Figure 12. UBE-1099 did not affect endothelin expression.

Supplemental Figure 13. Full-length blots for Figure 5, A and B.

References

- Baird L, Dinkova-Kostova AT: The cytoprotective role of the Keap1-Nrf2 pathway. *Arch Toxicol* 85: 241–272, 2011 <https://doi.org/10.1007/s00204-011-0674-5>
- Tebay LE, Robertson H, Durant ST, Vitale SR, Penning TM, Dinkova-Kostova AT, Hayes JD: Mechanisms of activation of the transcription factor Nrf2 by redox stressors, nutrient cues, and energy status and the pathways through which it attenuates degenerative disease. *Free Radic Biol Med* 88[Pt B]: 108–146, 2015 <https://doi.org/10.1016/j.freeradbiomed.2015.06.021>
- Kansanen E, Kuosmanen SM, Leinonen H, Levonen AL: The Keap1-Nrf2 pathway: Mechanisms of activation and dysregulation in cancer. *Redox Biol* 1: 45–49, 2013 <https://doi.org/10.1016/j.redox.2012.10.001>
- Canning P, Sorrell FJ, Bullock AN: Structural basis of Keap1 interactions with Nrf2. *Free Radic Biol Med* 88[Pt B]: 101–107, 2015 <https://doi.org/10.1016/j.freeradbiomed.2015.05.034>
- Baird L, Llères D, Swift S, Dinkova-Kostova AT: Regulatory flexibility in the Nrf2-mediated stress response is conferred by conformational cycling of the Keap1-Nrf2 protein complex. *Proc Natl Acad Sci U S A* 110: 15259–15264, 2013 <https://doi.org/10.1073/pnas.1305687110>
- Baird L, Swift S, Llères D, Dinkova-Kostova AT: Monitoring Keap1-Nrf2 interactions in single live cells. *Biotechnol Adv* 32: 1133–1144, 2014 <https://doi.org/10.1016/j.biotechadv.2014.03.004>
- Deshmukh P, Unni S, Krishnappa G, Padmanabhan B: The Keap1-Nrf2 pathway: Promising therapeutic target to counteract ROS-mediated damage in cancers and neurodegenerative diseases. *Biophys Rev* 9: 41–56, 2017 <https://doi.org/10.1007/s12551-016-0244-4>
- Magesh S, Chen Y, Hu L: Small molecule modulators of Keap1-Nrf2-ARE pathway as potential preventive and therapeutic agents. *Med Res Rev* 32: 687–726, 2012 <https://doi.org/10.1002/med.21257>
- Pergola PE, Raskin P, Toto RD, Meyer CJ, Huff JW, Grossman EB, Krauth M, Ruiz S, Audhya P, Christ-Schmidt H, Wittes J, Warnock DG; BEAM Study Investigators: Bardoxolone methyl and kidney function in CKD with type 2 diabetes. *N Engl J Med* 365: 327–336, 2011 <https://doi.org/10.1056/NEJMoa1105351>
- Nangaku M, Kanda H, Takama H, Ichikawa T, Hase H, Akiyama T: Randomized clinical trial on the effect of bardoxolone

- methyl on GFR in diabetic kidney disease patients (TSUBAKI Study). *Kidney Int Rep* 5: 879–890, 2020 <https://doi.org/10.1016/j.ekir.2020.03.030>
11. de Zeeuw D, Akizawa T, Audhya P, Bakris GL, Chin M, Christ-Schmidt H, Goldsberry A, Houser M, Krauth M, Lambers Heerspink HJ, McMurray JJ, Meyer CJ, Parving H-H, Remuzzi G, Toto RD, Vaziri ND, Wanner C, Wittes J, Wrolstad D, Chertow GM; BEACON Trial Investigators: Bardoxolone methyl in type 2 diabetes and Stage 4 chronic kidney disease. *N Engl J Med* 369: 2492–2503, 2013 <https://doi.org/10.1056/NEJMoa1306033>
 12. Chin MP, Reisman SA, Bakris GL, O'Grady M, Linde PG, McCullough PA, Packham D, Vaziri ND, Ward KW, Warnock DG, Meyer CJ: Mechanisms contributing to adverse cardiovascular events in patients with type 2 diabetes mellitus and Stage 4 chronic kidney disease treated with bardoxolone methyl. *Am J Nephrol* 39: 499–508, 2014 <https://doi.org/10.1159/000362906>
 13. Yamawaki K, Kanda H, Shimazaki R: Nrf2 activator for the treatment of kidney diseases. *Toxicol Appl Pharmacol* 360: 30–37, 2018 <https://doi.org/10.1016/j.taap.2018.09.030>
 14. Cuadrado A, Rojo AI, Wells G, Hayes JD, Cousin SP, Rumsey WL, Attucks OC, Franklin S, Levenon A-L, Kensler TW, Dinkova-Kostova AT: Therapeutic targeting of the NRF2 and KEAP1 partnership in chronic diseases. *Nat Rev Drug Discov* 18: 295–317, 2019 <https://doi.org/10.1038/s41573-018-0008-x>
 15. Pallesen JS, Tran KT, Bach A: Non-covalent small-molecule Kelch-like ECH-associated protein 1-nuclear factor erythroid 2-related factor 2 (Keap1-Nrf2) inhibitors and their potential for targeting central nervous system diseases. *J Med Chem* 61: 8088–8103, 2018 <https://doi.org/10.1021/acs.jmedchem.8b00358>
 16. Rush BM, Bondi CD, Stocker SD, Barry KM, Small SA, Ong J, Jobbagy S, Stolz DB, Bastacky SI, Chartoumpakis DV, Kensler TW, Tan RJ: Genetic or pharmacologic Nrf2 activation increases proteinuria in chronic kidney disease in mice. *Kidney Int* 99: 102–116, 2021 <https://doi.org/10.1016/j.kint.2020.07.036>
 17. Ding Y, Stidham RD, Bumeister R, Trevino I, Winters A, Sprouse M, Ding M, Ferguson DA, Meyer CJ, Wigley WC, Ma R: The synthetic triterpenoid, RTA 405, increases the glomerular filtration rate and reduces angiotensin II-induced contraction of glomerular mesangial cells. *Kidney Int* 83: 845–854, 2013 <https://doi.org/10.1038/ki.2012.393>
 18. Lu MC, Zhao J, Liu YT, Liu T, Tao MM, You QD, Jiang ZY: CPUY192018, a potent inhibitor of the Keap1-Nrf2 protein-protein interaction, alleviates renal inflammation in mice by restricting oxidative stress and NF- κ B activation. *Redox Biol* 26: 101266, 2019 <https://doi.org/10.1016/j.redox.2019.101266>
 19. Rheault MN, Kren SM, Thielen BK, Mesa HA, Crosson JT, Thomas W, Sado Y, Kashtan CE, Segal Y: Mouse model of X-linked Alport syndrome. *J Am Soc Nephrol* 15: 1466–1474, 2004 <https://doi.org/10.1097/01.ASN.0000130562.90255.8F>
 20. Yokota T, Omachi K, Suico MA, Kamura M, Kojima H, Fukuda R, Motomura K, Teramoto K, Kaseda S, Kuwazuru J, Takeo T, Nakagata N, Shuto T, Kai H: STAT3 inhibition attenuates the progressive phenotypes of Alport syndrome mouse model. *Nephrol Dial Transplant* 33: 214–223, 2018 <https://doi.org/10.1093/ndt/gfx246>
 21. Sannomiya Y, Kaseda S, Kamura M, Yamamoto H, Yamada H, Inamoto M, Kuwazuru J, Niino S, Shuto T, Suico MA, Kai H: The role of discoidin domain receptor 2 in the renal dysfunction of Alport syndrome mouse model. *Ren Fail* 43: 510–519, 2021 <https://doi.org/10.1080/0886022X.2021.1896548>
 22. Omachi K, Kaseda S, Yokota T, Kamura M, Teramoto K, Kuwazuru J, Kojima H, Nohara H, Koyama K, Ohtsuki S, Misumi S, Takeo T, Nakagata N, Li JD, Shuto T, Suico MA, Miner JH, Kai H: Metformin ameliorates the severity of experimental Alport syndrome. *Sci Rep* 11: 7053, 2021 <https://doi.org/10.1038/s41598-021-86109-1>
 23. Yokota T, Omachi K, Suico MA, Kojima H, Kamura M, Teramoto K, Kaseda S, Kuwazuru J, Shuto T, Kai H: Bromide supplementation exacerbated the renal dysfunction, injury and fibrosis in a mouse model of Alport syndrome. *PLoS One* 12: e0183959, 2017 <https://doi.org/10.1371/journal.pone.0183959>
 24. Koga T, Kai Y, Fukuda R, Morino-Koga S, Suico MA, Koyama K, Sato T, Shuto T, Kai H: Mild electrical stimulation and heat shock ameliorates progressive proteinuria and renal inflammation in mouse model of Alport syndrome. *PLoS One* 7: e43852, 2012 <https://doi.org/10.1371/journal.pone.0043852>
 25. Schock-Kusch D, Geraci S, Ermeling E, Shulhevich Y, Sticht C, Hesser J, Stsepankou D, Neudecker S, Pill J, Schmitt R, Melk A: Reliability of transcutaneous measurement of renal function in various strains of conscious mice. *PLoS One* 8: e71519, 2013 <https://doi.org/10.1371/journal.pone.0071519>
 26. Davies TG, Wixted WE, Coyle JE, Griffiths-Jones C, Hearn K, McMenamin R, Norton D, Rich SJ, Richardson C, Saxty G, Willems HMG, Woolford AJA, Cottom JE, Kou JP, Yonchuk JG, Feldser HG, Sanchez Y, Foley JP, Bolognese BJ, Logan G, Hessel PL, Yan H, Callahan JF, Heightman TD, Kerns JK: Monoacidic inhibitors of the Kelch-like ECH-associated protein 1: Nuclear factor erythroid 2-related factor 2 (KEAP1:NRF2) protein-protein interaction with high cell potency identified by fragment-based discovery. *J Med Chem* 59: 3991–4006, 2016 <https://doi.org/10.1021/acs.jmedchem.6b00228>
 27. Rossing P, Block GA, Chin MP, Goldsberry A, Heerspink HJL, McCullough PA, Meyer CJ, Packham D, Pergola PE, Spinowitz B, Sprague SM, Warnock DG, Chertow GM: Effect of bardoxolone methyl on the urine albumin-to-creatinine ratio in patients with type 2 diabetes and Stage 4 chronic kidney disease. *Kidney Int* 96: 1030–1036, 2019 <https://doi.org/10.1016/j.kint.2019.04.027>
 28. Lu CC, Wang GH, Lu J, Chen PP, Zhang Y, Hu ZB, Ma KL: Role of podocyte injury in glomerulosclerosis. *Adv Exp Med Biol* 1165: 195–232, 2019 https://doi.org/10.1007/978-981-13-8871-2_10
 29. Ning L, Suleiman HY, Miner JH: Synaptopodin is dispensable for normal podocyte homeostasis but is protective in the context of acute podocyte injury. *J Am Soc Nephrol* 31: 2815–2832, 2020 <https://doi.org/10.1681/ASN.2020050572>
 30. Ning L, Suleiman HY, Miner JH: Synaptopodin deficiency exacerbates kidney disease in a mouse model of Alport Syndrome. *Am J Physiol Physiol* 321: F12–F25, 2021 <https://doi.org/ajrenal.00035.2021>
 31. Rapa SF, Di Iorio BR, Campiglia P, Heidland A, Marzocco S: Inflammation and oxidative stress in chronic kidney disease—Potential therapeutic role of minerals, vitamins and plant-derived metabolites. *Int J Mol Sci* 21: 263, 2019 <https://doi.org/10.3390/ijms21010263>
 32. Ling XC, Kuo K-L: Oxidative stress in chronic kidney disease. *Renal Replace Ther* 4: 53, 2018 <https://doi.org/10.1186/s41100-018-0195-2>
 33. Homma S, Ishii Y, Morishima Y, Yamadori T, Matsuno Y, Hara-guchi N, Kikuchi N, Satoh H, Sakamoto T, Hizawa N, Itoh K, Yamamoto M: Nrf2 enhances cell proliferation and resistance to anticancer drugs in human lung cancer. *Clin Cancer Res* 15: 3423–3432, 2009 <https://doi.org/10.1158/1078-0432.CCR-08-2822>
 34. Reddy NM, Kleeberger SR, Bream JH, Fallon PG, Kensler TW, Yamamoto M, Reddy SP: Genetic disruption of the Nrf2 compromises cell-cycle progression by impairing GSH-induced redox signaling. *Oncogene* 27: 5821–5832, 2008 <https://doi.org/10.1038/onc.2008.188>
 35. Márton M, Tihanyi N, Gyulavári P, Bánhegyi G, Kapuy O: NRF2-regulated cell cycle arrest at early stage of oxidative stress response mechanism. *PLoS One* 13: e0207949, 2018 <https://doi.org/10.1371/journal.pone.0207949>
 36. Ko E, Kim D, Min DW, Kwon SH, Lee JY: Nrf2 regulates cell motility through RhoA-ROCK1 signalling in non-small-cell lung cancer cells. *Sci Rep* 11: 1247, 2021 <https://doi.org/10.1038/s41598-021-81021-0>
 37. Dinkova-Kostova AT, Abramov AY: The emerging role of Nrf2 in mitochondrial function. *Free Radic Biol Med* 88[Pt B]: 179–188, 2015 <https://doi.org/10.1016/j.freeradbiomed.2015.04.036>
 38. Holmström KM, Kostov RV, Dinkova-Kostova AT: The multifaceted role of Nrf2 in mitochondrial function. *Curr Opin Toxicol* 1: 80–91, 2016 <https://doi.org/10.1016/j.cotox.2016.10.002>
 39. Fortner KA, Blanco LP, Buskiewicz I, Huang N, Gibson PC, Cook DL, Pedersen HL, Yuen PST, Murphy MP, Perl A, Kaplan MJ, Budd RC: Targeting mitochondrial oxidative stress with

- MitoQ reduces NET formation and kidney disease in lupus-prone MRL-*lpr* mice [published correction appears in *Lup Sci Med* 7: E000387corr1, 2020 10.1136/lupus-2020-000387corr1]. *Lupus Sci Med* 7: e000387, 2020 <https://doi.org/10.1136/lupus-2020-000387>
40. Xiao L, Xu X, Zhang F, Wang M, Xu Y, Tang D, Wang J, Qin Y, Liu Y, Tang C, He L, Greka A, Zhou Z, Liu F, Dong Z, Sun L: The mitochondria-targeted antioxidant MitoQ ameliorated tubular injury mediated by mitophagy in diabetic kidney disease via Nrf2/PINK1. *Redox Biol* 11: 297–311, 2017 <https://doi.org/10.1016/j.redox.2016.12.022>
 41. Wu T, Ye Y, Min SY, Zhu J, Khobahy E, Zhou J, Yan M, Hemachandran S, Pathak S, Zhou XJ, Andreeff M, Mohan C: Prevention of murine lupus nephritis by targeting multiple signaling axes and oxidative stress using a synthetic triterpenoid. *Arthritis Rheumatol* 66: 3129–3139, 2014 <https://doi.org/10.1002/art.38782>
 42. Camer D, Yu Y, Szabo A, Wang H, Dinh CHL, Huang XF: Bardoxolone methyl prevents the development and progression of cardiac and renal pathophysiology in mice fed a high-fat diet. *Chem Biol Interact* 243: 10–18, 2016 <https://doi.org/10.1016/j.cbi.2015.11.018>
 43. Aminzadeh MA, Reisman SA, Vaziri ND, Khazaeli M, Yuan J, Meyer CJ: The synthetic triterpenoid RTA dh404 (CDDO-dhTFA) restores Nrf2 activity and attenuates oxidative stress, inflammation, and fibrosis in rats with chronic kidney disease. *Xenobiotica* 44: 570–578, 2014 <https://doi.org/10.3109/00498254.2013.852705>
 44. Zoja C, Corna D, Nava V, Locatelli M, Abbate M, Gaspari F, Carrara F, Sangalli F, Remuzzi G, Benigni A: Analogs of bardoxolone methyl worsen diabetic nephropathy in rats with additional adverse effects. *Am J Physiol Renal Physiol* 304: F808–F819, 2013 <https://doi.org/10.1152/ajprenal.00376.2012>
 45. Gross O, Licht C, Anders HJ, Hoppe B, Beck B, Tönshoff B, Höcker B, Wygoda S, Ehrich JHH, Pape L, Konrad M, Rascher W, Dötsch J, Müller-Wiefel DE, Hoyer P, Knebelmann B, Pirson Y, Grunfeld JP, Niaudet P, Cochat P, Heidet L, Lebbah S, Torra R, Friede T, Lange K, Müller GA, Weber M; Study Group Members of the Gesellschaft für Pädiatrische Nephrologie: Early angiotensin-converting enzyme inhibition in Alport syndrome delays renal failure and improves life expectancy. *Kidney Int* 81: 494–501, 2012 <https://doi.org/10.1038/ki.2011.407>
 46. Fernandez-Fernandez B, Sarafidis P, Kanbay M, Navarro-González JF, Soler MJ, Górriz JL, Ortiz A: SGLT2 inhibitors for non-diabetic kidney disease: Drugs to treat CKD that also improve glycaemia. *Clin Kidney J* 13: 728–733, 2020 <https://doi.org/10.1093/ckj/sfaa198>
 47. Zhao S, Lo CS, Miyata KN, Ghosh A, Zhao XP, Chenier I, Cailhier JF, Ethier J, Lattouf JB, Filep JG, Ingelfinger JR, Zhang SL, Chan JSD: Overexpression of Nrf2 in renal proximal tubular cells stimulates sodium-glucose cotransporter 2 expression and exacerbates dysglycemia and kidney injury in diabetic mice. *Diabetes* 70: 1388–1403, 2021 <https://doi.org/10.2337/db20-1126>
 48. Mann JFE, Green D, Jamerson K, Ruilope LM, Kuranoff SJ, Littke T, Viberti G; ASCEND Study Group: Avosentan for overt diabetic nephropathy. *J Am Soc Nephrol* 21: 527–535, 2010 <https://doi.org/10.1681/ASN.2009060593>

Received: July 12, 2021 **Accepted:** November 29, 2021